

*Supporting Information for*

## **Chemical exchange of labile protons by deuterium enables selective detection of pharmaceuticals in solid formulations**

Claire Welton<sup>‡a</sup>, Parth Raval<sup>‡a</sup>, Julien Trébosc<sup>b</sup>, and G. N. Manjunatha Reddy<sup>a\*</sup>

<sup>a</sup> *University of Lille, CNRS, Centrale Lille Institut, Univ. Artois, UMR 8181–UCCS– Unité de Catalyse et Chimie du Solide, F-59000, Lille, France.*

<sup>b</sup> *University of Lille, CNRS, INRAE, Centrale Lille, Univ. Artois, FR 2638 - IMEC - Institut Michel-Eugène Chevreul, F-59000 Lille, France.*

<sup>‡</sup> *Contributed equally to this work*

\*Corresponding author: [gnm.reddy@univ.lille.fr](mailto:gnm.reddy@univ.lille.fr)

### **Table of contents**

1. Synthesis and experimental details
2. Estimation of the extent of deuteration (%) in molecular solids
3. 1D <sup>1</sup>H and <sup>2</sup>H MAS NMR spectra of partially deuterated samples acquired at 9.4 T and 18.8 T
4. Analysis of <sup>2</sup>H NMR spectra of L-histidine.HCl.H<sub>2</sub>O
5. 1D NMR of solid-state formulation of L-histidine.HCl.H<sub>2</sub>O and microcrystalline cellulose
6. Analysis of 1D <sup>2</sup>H NMR spectra of dopamine.HCl
7. 2D <sup>2</sup>H-<sup>1</sup>H iCOSY spectra of dopamine.HCl
8. Packing interactions in dopamine.HCl
9. References

## 1. Synthesis and experimental details

**Partial deuteration of labile protons in molecular solids.** Powders of L-histidine·HCl·H<sub>2</sub>O [C<sub>6</sub>H<sub>9</sub>N<sub>3</sub>O<sub>2</sub>·HCl·H<sub>2</sub>O], dopamine·HCl [(HO)<sub>2</sub>C<sub>6</sub>H<sub>3</sub>(CH<sub>2</sub>)<sub>2</sub>NH<sub>2</sub>·HCl] and microcrystalline cellulose (particle size, 20 μm) were purchased from Sigma Aldrich and used as received. The solubility of histidine is 50 mg/mL, and dopamine is 600 mg/mL in water, whereas microcrystalline cellulose is relatively insoluble in water and sparingly soluble in dilute acids and weak bases (e.g., NaOH solution). Approximately 10 mg of L-histidine·HCl·H<sub>2</sub>O [C<sub>6</sub>H<sub>9</sub>N<sub>3</sub>O<sub>2</sub>·HCl·H<sub>2</sub>O] and dopamine·HCl [(HO)<sub>2</sub>C<sub>6</sub>H<sub>3</sub>(CH<sub>2</sub>)<sub>2</sub>NH<sub>2</sub>·HCl] powders were dissolved in 500 microliters of D<sub>2</sub>O in a vial. For the blends, the powders of L-histidine·HCl·H<sub>2</sub>O (20 wt.%) and dopamine·HCl (5-30 wt.%) were separately mixed with microcrystalline cellulose (MCC), and dissolved in 500 microliters of D<sub>2</sub>O. These suspensions were allowed for sonication/agitation in order to dissociate large lumps of powder (if any) and to ensure complete dissolution of APIs. Solutions were transferred into separate petri dishes and allowed to settle overnight at room temperature. After solvent evaporation, the fine powders of partially deuterated samples were scratched from the petri dish to collect enough material for ssNMR experiments. For the high-temperature H/D exchange experiment, powders of L-histidine·HCl·H<sub>2</sub>O, and dopamine·HCl were dissolved in 500 microliters of D<sub>2</sub>O in a petri dish. These suspensions were heated at 100 (±3) °C in order to facilitate the H/D exchange until evaporation of solvent and gradually cooled down to room temperature. Fine dry powders were formed within a few minutes. The same procedure was applied to the solid formulations. For all neat compounds and blends, the extent of deuteration is estimated by analysing 1D <sup>1</sup>H NMR spectra by comparing the relative integrals of the labile proton sites in pristine and deuterated samples.

**Solid-state NMR spectroscopy.** For the analysis of pristine compounds, all samples were used as received. Approximately 2.2 mg of each powder was packed into a 1.3 mm (outer diameter) rotor. All 1D <sup>1</sup>H MAS NMR experiments were carried out either on a 9.4 T, 18.8 T, or on a 28.2 T Bruker Avance NEO4 solid-state NMR spectrometer operating at a <sup>1</sup>H Larmor frequency of 400.1 MHz, 800.1 MHz or 1200.5 MHz. Each of them was equipped with a 1.3 mm double-resonance MAS probe head. All 2D <sup>1</sup>H-<sup>2</sup>H isotope correlation experiments were performed on a 18.8 T with 60 kHz MAS. The <sup>1</sup>H and <sup>2</sup>H pulse lengths and dipolar recoupling periods ( $\tau_{\text{rcpl}}$ ) were empirically optimized using 1D versions of the D-HMQC pulse sequence. 1D <sup>1</sup>H MAS NMR spectra of neat compounds and blends were acquired with 32 coadded transients with a recycle delay of 10 s, leading to an experimental time of 6 mins each. All <sup>2</sup>H MAS NMR spectra were acquired by coaddition of 1024 transients, leading to an experimental time of 16 mins each. <sup>2</sup>H MAS NMR spectra can be acquired with 96 coadded transients in under a minute. All <sup>1</sup>H chemical shifts are calibrated with respect to neat TMS using adamantane as an external reference (<sup>1</sup>H resonance, 1.85 ppm). All the <sup>2</sup>H shifts are calibrated with respect to TMS using liquid D<sub>2</sub>O as an external reference (<sup>2</sup>H resonance, 4.80 ppm).

**Isotope correlation spectroscopy (iCOSY).** Benefiting from the high sensitivity, <sup>1</sup>H ssNMR experiments provide an efficient method for the rapid characterization of low drug load formulations. If one or more <sup>1</sup>H peaks of APIs are resolved, then the characteristics of <sup>1</sup>H NMR spectra of APIs in pharmaceutical formulations can be obtained by using combinations of frequency-selective saturation and excitation pulses, and 2D <sup>1</sup>H spin diffusion experiments.<sup>1</sup> To gain insight into the local structures and interactions in partially deuterated compounds, we carried out 2D <sup>1</sup>H-<sup>2</sup>H heteronuclear multiple-quantum coherence (HMQC) experiments. The pulse sequence used to acquire the <sup>2</sup>H-<sup>1</sup>H HMQC spectra is reported in **Figure S1**. An example of pulse program suitable for Bruker spectrometers is provided in a previous study<sup>2</sup> (see: supporting information of Ref. 2).

All 2D NMR experiments were performed on a Bruker Avance Neo (18.8 T Larmor frequency of <sup>1</sup>H = 800.1 MHz, <sup>2</sup>H = 122.8 MHz) spectrometer, using a 1.3 mm Bruker probe operating in double-resonance mode at a 60 kHz MAS frequency. SR4<sub>1</sub><sup>2</sup> recoupling elements were used to reintroduce the heteronuclear <sup>2</sup>H-<sup>1</sup>H dipolar

couplings, using a recoupling duration  $\tau_{\text{rcpl}} = 166$  microseconds. The  $^1\text{H}$  90-degree pulse duration and the  $^2\text{H}$  pulse durations were  $2.2 \mu\text{s}$  and  $16.6 \mu\text{s}$ , respectively. For a L-histidine.HCl.H<sub>2</sub>O, 80  $t_1$  FIDs were acquired using the States method to achieve sign discrimination in  $F_1$  with a rotor synchronized increment of  $16.6 \mu\text{s}$ , 32 transients were coadded with a recycle delay of 6 s, corresponding to a total experimental time of 4.2 h. For L-histidine.HCl.H<sub>2</sub>O/microcrystalline cellulose blend (20/80 wt.%), 120  $t_1$  FIDs were acquired using the States method to achieve sign discrimination in  $F_1$  with a rotor synchronized increment of  $16.6 \mu\text{s}$ , 32 transients were coadded with a recycle delay of 6 s, corresponding to a total experimental time of  $\sim 7$  h. For dopamine.HCl, 64  $t_1$  FIDs were acquired using the States method to achieve sign discrimination in  $F_1$  with a rotor synchronized increment of  $16.6 \mu\text{s}$ , 8 transients were coadded with a recycle delay of 5 s, corresponding to a total experimental time of  $\sim 1.5$  h. For the 30 wt.% dopamine.HCl blend with microcrystalline cellulose, 96  $t_1$  FIDs were acquired using the States method to achieve sign discrimination in  $F_1$  with a rotor synchronized increment of  $16.6 \mu\text{s}$ . 24 transients were coadded with a recycle delay of 5 s, corresponding to a total experimental time of  $\sim 4$  h.

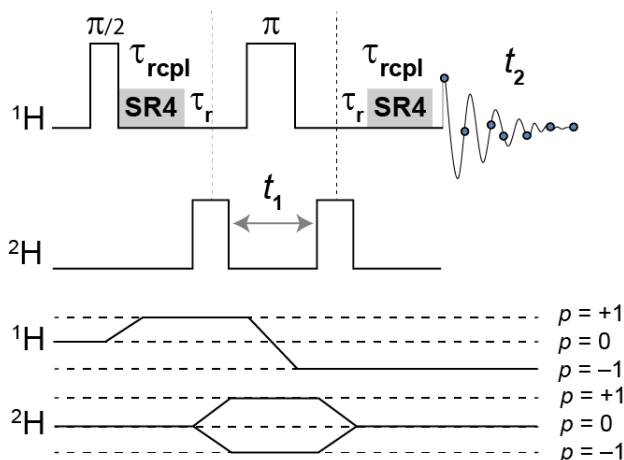


**Figure S1.** Schematic of HMQC pulse sequence (top) used in the present study to acquire 1D  $^2\text{H}$ -filtered MAS and 2D iCOSY spectra. SR4<sub>1</sub><sup>2</sup> pulses are applied for the recoupling of  $^1\text{H}$ - $^2\text{H}$  dipolar interactions. The evolution during  $t_1$ , the recoupling pulses, and  $^2\text{H}$  pulses are rotor synchronized with respect to the sample spinning. The coherence pathways are provided at the bottom.

**First-principles calculations using a periodic-DFT approach.** For calculations, input files were generated by taking molecular coordinates from previously published crystal structures deposited in the Cambridge database: L-histidine.HCl.H<sub>2</sub>O (CCDC code: HISTCMO1)<sup>3</sup> and dopamine.HCl (CCDC code: DOPAMN).<sup>4</sup> All calculations were performed using the CASTEP 19.11 code.<sup>5</sup> Geometry optimization was carried out using periodic density functional theory (DFT), and the NMR chemical shifts were computed using the gauge including projected augmented wave (GIPAW) method as described by Pickard and Mauri.<sup>6,7</sup> The generalized density approximation DFT functional PBE (Perdew-Burke Ernzerhof) with the Tkatchenko-Scheffler (TS) dispersion correction scheme (DFT-D method) was applied with ultrasoft pseudopotentials.<sup>8,9</sup> The Broyden-Fletcher-Goldfarb-Shanno (BESG) optimization algorithm was used to geometry optimize unconstrained molecular systems. The Monkhorst-Pack grid of minimum sample spacing  $0.07 \times 2\pi \text{ \AA}^{-1}$  was applied to sample the Brillouin zone (i.e., primitive cell in reciprocal space). The molecular geometry was converged with a maximum plane wave cut-off energy of 23.15 Hartrees. The atom positions in the unit cell were allowed to relax within the unit cell until the average forces, energies, and displacements remaining were below  $3.6749 \times 10^{-7}$  Hartree/ $\text{\AA}$ , 0.0011025 Hartrees, and 0.001  $\text{\AA}$ , respectively. For L-histidine.HCl.H<sub>2</sub>O, and dopamine.HCl, all interatomic distances stated in this study correspond to the DFT optimized structures.<sup>10</sup>

## 2. Estimation of the extent of deuteration (%) in molecular solids

**Figure S2** presents the 1D  $^1\text{H}$  spectrum before and after deuteration (at room temperature) of molecular solids utilized in this work, along with their 1D  $^2\text{H}$  spectrum post-deuteration. For overlapping sites, the proton integral values are measured by spectral deconvolution analysis. The  $^1\text{H}$  MAS spectra are presented by normalizing the peak intensities of  $\text{CH}_2$  and  $\text{CH}$  (H2,3,4) sites for L-histidine.HCl.H<sub>2</sub>O, and  $\text{CH}_2$  sites (H2,2', 3, 3') for dopamine.HCl, in order to see the intensity losses for NH, NH<sub>3</sub>, OH, and H<sub>2</sub>O sites.

The extent of deuteration,  $D(\%)$ , was estimated by comparing the  $^1\text{H}$  integral values of each labile proton site in pristine and deuterated samples using Equation 1, where  $I_{\text{H}}$  (pristine) and  $I_{\text{H}}$  (deuterated) are the peak integrals of labile protons in pristine and deuterated samples.

$$D(\%) = \frac{I_{\text{H}}(\text{deuterated})}{I_{\text{H}}(\text{pristine})} 100 \quad (1)$$

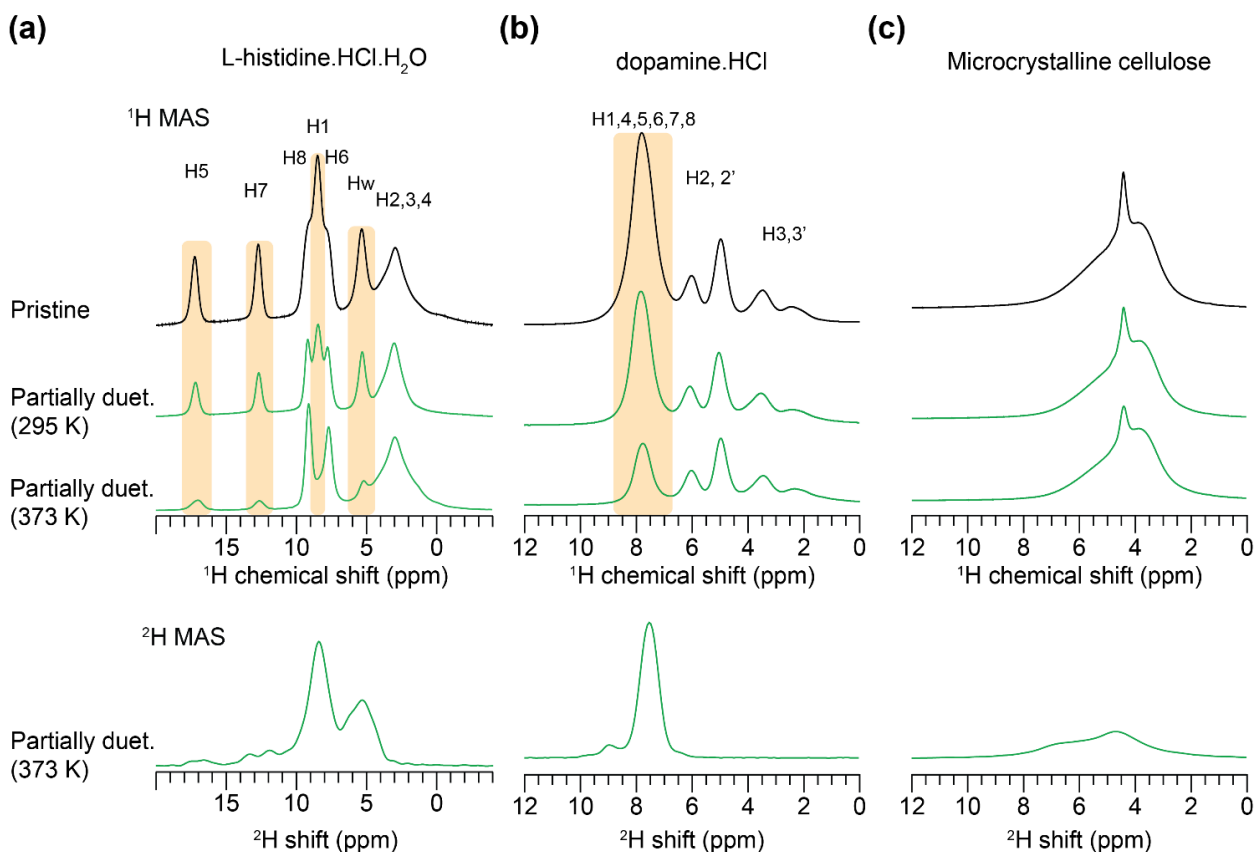


**Figure S2.** Solid-state 1D  $^1\text{H}$  MAS (top) spectra of pristine (black) and partially deuterated samples at different temperatures (green) together with the  $^2\text{H}$  MAS (bottom) spectra: (a) L-histidine.HCl.H<sub>2</sub>O (b) dopamine.HCl (c) microcrystalline cellulose. Vertical yellow bands indicate the peaks of labile protons that undergo exchange with deuterium. All spectra were acquired at 18.8 T (Larmor frequency of  $^1\text{H}$  = 800.1 MHz) with 60 kHz MAS.

### 3. 1D $^1\text{H}$ and $^2\text{H}$ MAS NMR spectra of partially deuterated samples acquired at 9.4 T and 18.8 T

For partially deuterated L-histidine.HCl.H<sub>2</sub>O, and dopamine.HCl,  $^1\text{H}$  and  $^2\text{H}$  MAS spectra acquired at different magnetic field strengths such as 9.4 T (400.1 MHz) and 18.8 T (800.1 MHz) are presented in Figure 3. All spectra were acquired at 60 kHz MAS to maintain a consistent spinning speed. Resolution and sensitivity enhancements in the  $^1\text{H}$  MAS spectra obtained at 18.8 T are evident from relatively better-resolved peaks, for example, in the 6-10 ppm range for L-histidine.HCl.H<sub>2</sub>O as well in the 4-10 ppm range for dopamine.HCl. The resolution of the  $^2\text{H}$  MAS spectrum of L-histidine.HCl.H<sub>2</sub>O is dramatically improved by going from 9.4 T to 18.8 T, due to the well-known effect that the quadrupolar interaction scales inversely with the magnetic field strength. Therefore, a high magnetic field improves the resolution in  $^1\text{H}$  as well as in  $^2\text{H}$  MAS NMR spectra, enabling better resolution to be achieved in the 2D  $^1\text{H}$ - $^2\text{H}$  iCOSY spectra.

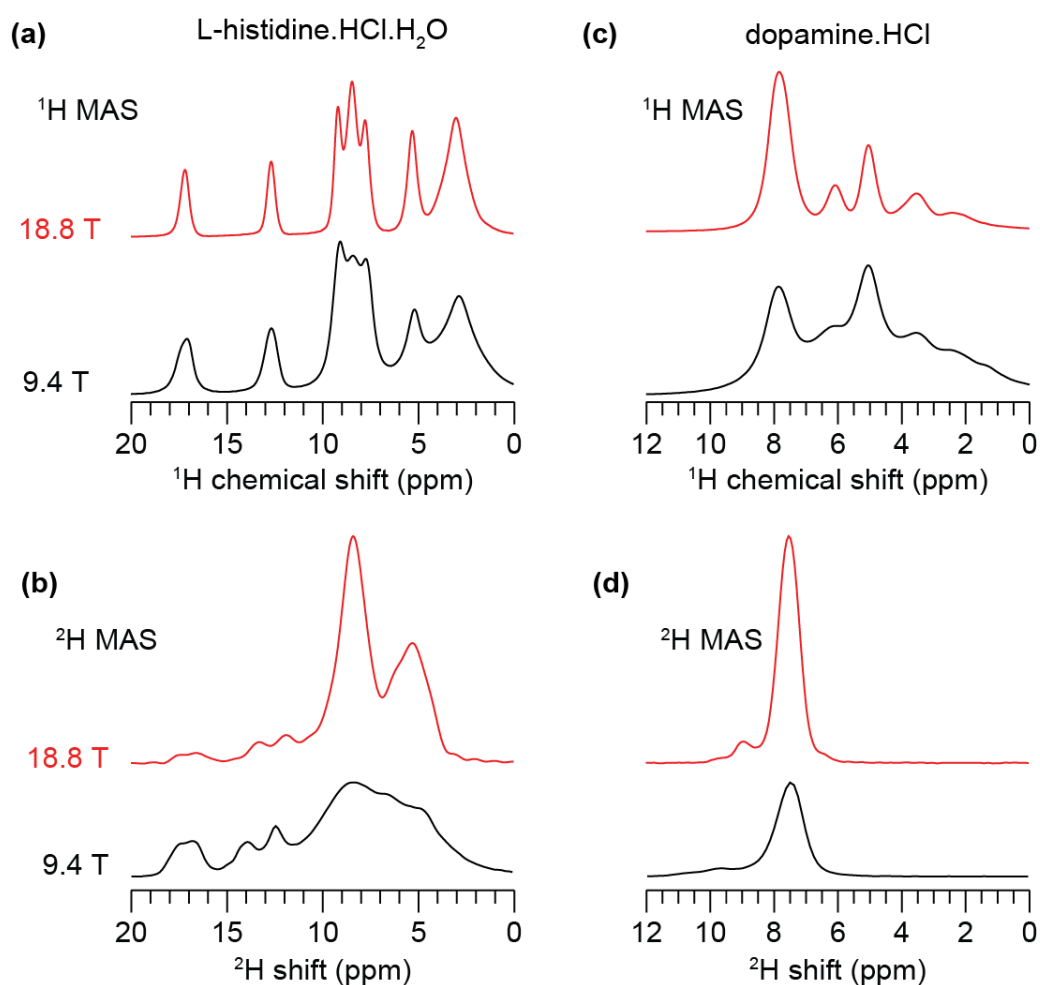


**Figure S3.** Solid-state 1D (a)  $^1\text{H}$  and (b)  $^2\text{H}$  MAS NMR spectra of L-histidine.HCl.H<sub>2</sub>O, and (b) and (c) are the same spectra of dopamine.HCl, respectively. All spectra were acquired at 9.4 T (blue) and 18.8 T (red) with 60 kHz MAS with  $^1\text{H}$  Larmor frequencies of 400.1 MHz (9.4 T) and 800.1 MHz (18.8 T) to compare the sensitivity and resolution.

#### 4. Analysis of $^2\text{H}$ NMR spectra of L-histidine.HCl.H $_2\text{O}$

In small organic molecules,  $^2\text{H}$  (spin  $I=1$ ) sites exhibit moderate quadrupole interactions (less than 1 MHz), leading to the spectra patterns which are several 100's ppm wide for non-spinning samples, i.e., much broader than the isotropic chemical shifts (a few 10's ppm). A high magnetic field strength in conjunction with fast MAS dramatically improves the resolution in  $^2\text{H}$  NMR spectra (**Figure S4**), allowing the isotropic chemical shifts and quadrupolar interactions to be measured and compared for different sites (**Figure S5**, and **Table S1**).

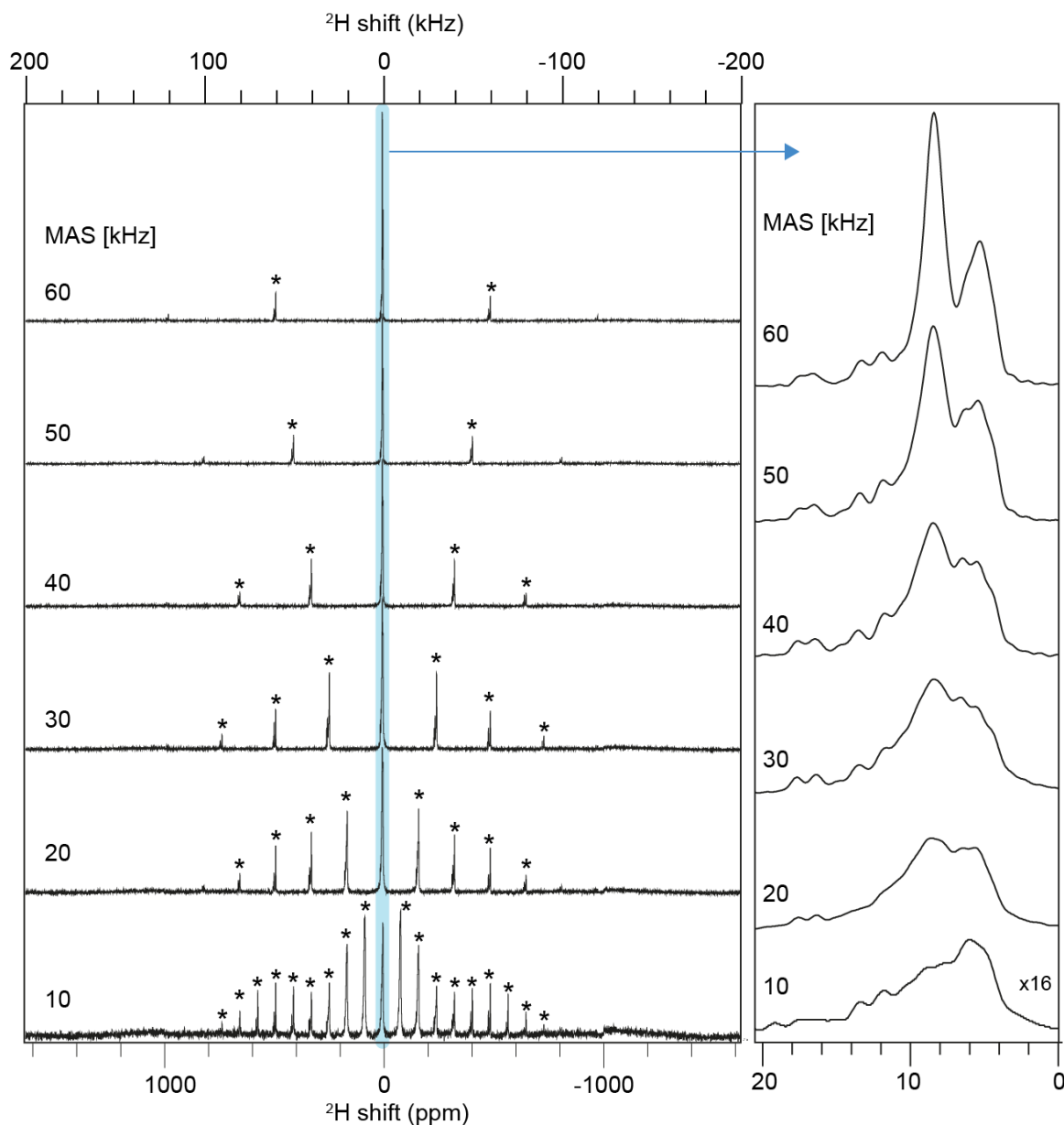


**Figure S4.** Solid-state 1D  $^2\text{H}$  MAS NMR spectra of L-histidine.HCl.H $_2\text{O}$  (left) with full spinning sideband patterns acquired at 18.8 T (Larmor frequency of  $^1\text{H}$  = 800.1 MHz and  $^2\text{H}$  = 122.8 MHz) with variable spinning frequencies as indicated. Spinning sidebands are denoted by asterisks. The expanded regions of  $^2\text{H}$  MAS spectra (0-20 ppm) are shown in the right-hand side panel, whereby line narrowing of -ND, -ND $_3$ , and -OD peaks is observed.

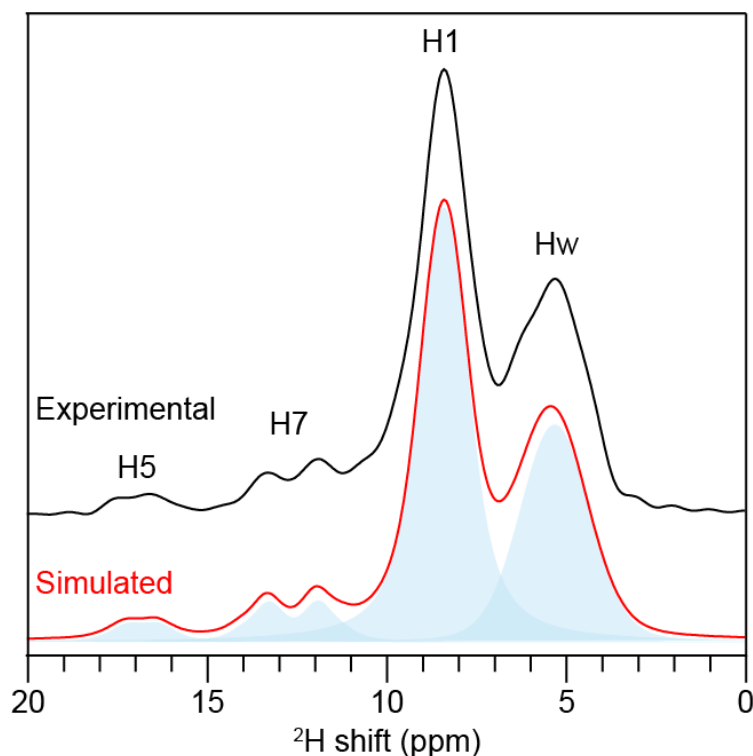


**Figure S5.** Lineshape analysis of a 1D  $^2\text{H}$  NMR spectrum of L-histidine.HCl.H<sub>2</sub>O acquired at 18.8 T (Larmor frequency of  $^1\text{H}$  = 800.1 MHz and  $^2\text{H}$  = 122.8 MHz) with 60 kHz MAS.

**Table S1.** GIPAW DFT calculated  $^2\text{H}$  electric field gradient tensors and quadrupolar parameters of partially deuterated NH and NH<sub>3</sub> sites in L-histidine.HCl.H<sub>2</sub>O along with experimental quadrupolar parameters obtained by lineshape fitting. <sup>a</sup>

$^2\text{H}$ site	GIPAW-DFT calculated						Experimental		
	$V_{xx}$	$V_{yy}$	$V_{zz}$	$C_Q$ (MHz)	$\eta_Q$	$\delta_{iso}$ (ppm)	$C_Q$ (MHz)	$\eta_Q$	$\delta_{iso}$ (ppm)
H5	-0.063	-0.094	0.157	0.11	0.20	17.9	0.14	0.11	16.8
H7	-0.120	-0.149	0.269	0.11	0.59	13.0	0.20	0.13	12.4
NH <sub>3</sub>	-0.117	0.315	0.246	0.16	0.05	8.1	0.05	0.14	8.3
H <sub>2</sub> O	-0.150	-0.200	0.350	0.22	0.13	4.9	0.14	0.12	5.3
CH <sub>2</sub>	-0.130	-0.530	0.270	0.17	0.06	2.4	---	---	---
CH	-0.120	-0.140	0.260	0.18	0.06	2.0	---	---	---

<sup>a</sup> Errors associated with the  $\delta_{iso}$ ,  $C_Q$ , and  $\eta_Q$  are estimated to be  $\pm 0.1$  ppm,  $\pm 0.04$  MHz, and  $\pm 0.03$ , respectively.

## 5. 1D NMR of solid-state formulation of L-histidine.HCl.H<sub>2</sub>O and microcrystalline cellulose

Presented in **Figure S6** are the <sup>1</sup>H MAS spectra of pristine and partially deuterated (green) histidine-cellulose blends, where the peaks corresponding to the heterocycle and NH<sub>3</sub> are resolved, but CH<sub>2</sub> and H<sub>w</sub> sites are overlapped with the proton peaks from cellulose. Nonetheless, intensity losses for H5,H7 and H1 peaks are observed. In the 1D <sup>2</sup>H-filtered <sup>1</sup>H NMR spectrum (blue) of the partially deuterated blend, the NH<sub>1</sub> and water peaks are resolved. This is further reflected in the <sup>2</sup>H MAS NMR spectrum for the blend (green, bottom). Poor resolution in the <sup>2</sup>H MAS NMR spectrum is due to the data acquired at a low field (9.4 T, <sup>1</sup>H = 400 MHz).

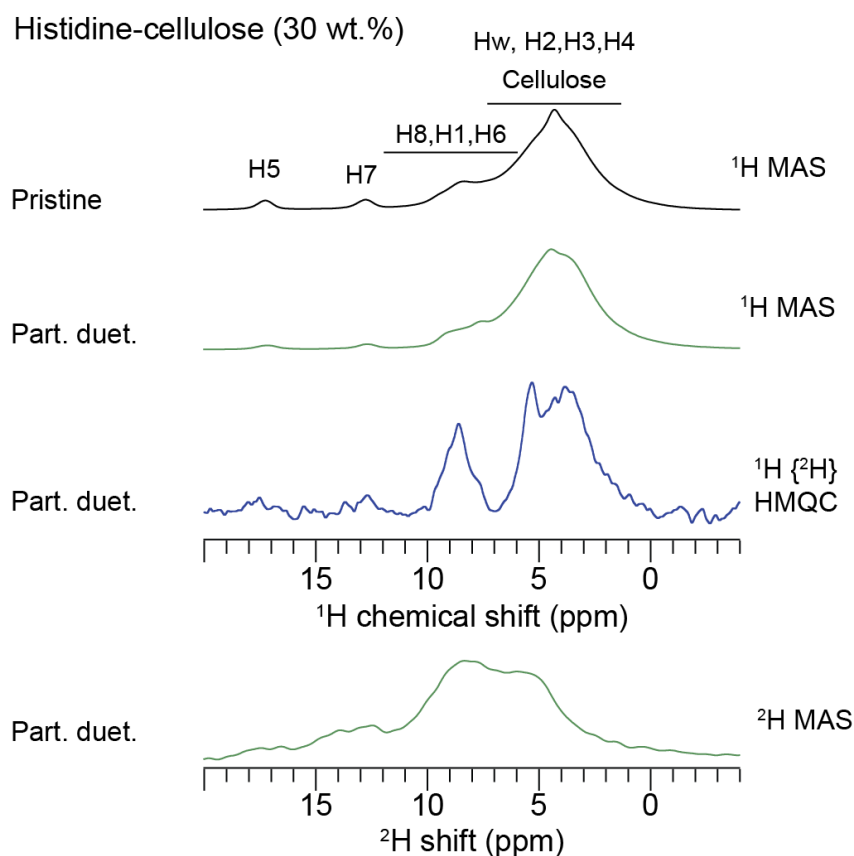


**Figure S6.** Solid-state 1D <sup>1</sup>H (top) and <sup>2</sup>H (bottom) spectra of pristine (black) and partially deuterated (green) solid-state formulation of L-histidine.HCl.H<sub>2</sub>O (20wt.%) and microcrystalline cellulose (80 wt.%) acquired at 9.4 T and 60 kHz.



## 6. Analysis of $^2\text{H}$ NMR spectra of dopamine.HCl

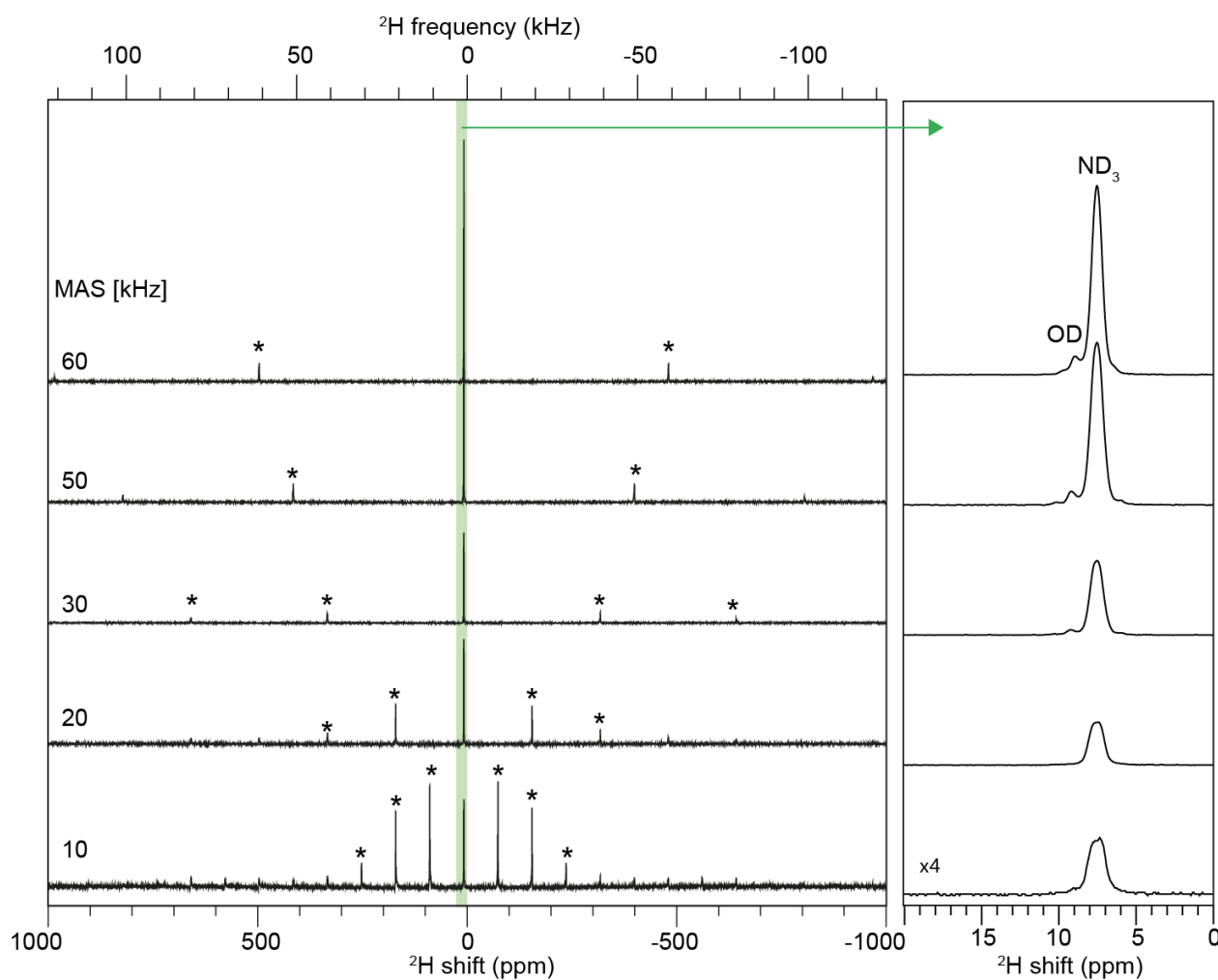


**Figure S7.** 1D  $^2\text{H}$  NMR spectra of dopamine-HCl (left) acquired at 18.8 T (Larmor frequency of  $^1\text{H}$  = 800.1 MHz and  $^2\text{H}$  = 122.8 MHz) at variable MAS as indicated alongside the spectrum. Spinning sidebands are denoted by asterisks. The expanded regions of  $^2\text{H}$  MAS spectra (0-20 ppm) are shown in the right-hand side panel, whereby line narrowing of  $\text{ND}_3$  and OD peaks are observed, enabling the resolution of -OD sites at > 40 kHz MAS.

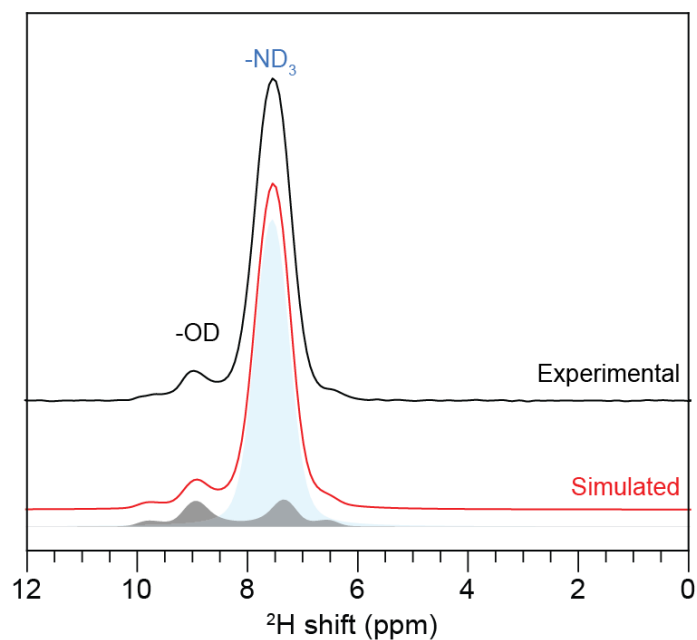


**Figure S8.** Lineshape analysis of 1D  $^2\text{H}$  NMR spectrum of dopamine.HCl acquired at 18.8 T (Larmor frequency of  $^1\text{H}$  = 800.1 MHz and  $^2\text{H}$  = 122.8 MHz) with 60 kHz MAS.

**Table S2.** GIPAW DFT calculated  $^2\text{H}$  electric field gradient tensors and quadrupolar parameters of partially deuterated  $\text{NH}_3$  sites in dopamine.HCl along with experimental quadrupolar parameters obtained by lineshape fitting.<sup>a</sup>

$^2\text{H}$ site	GIPAW-DFT calculated					Experimental			
	$V_{xx}$	$V_{yy}$	$V_{zz}$	$C_Q$ (MHz)	$\eta_Q$	$\delta_{iso}$ (ppm)	$C_Q$ (MHz)	$\eta_Q$	$\delta_{iso}$ (ppm)
$\text{ND}_3$	-0.131	-0.144	0.275	0.18	0.05	7.3	0.04	0.05	7.5
OD	-0.152	-0.195	0.347	0.23	0.12	7.5	0.21	0.17	7.9

<sup>a</sup> Errors associated with the  $\delta_{iso}$ ,  $C_Q$ , and  $\eta_Q$  are estimated to be  $\pm 0.1$  ppm,  $\pm 0.04$  MHz, and  $\pm 0.03$ , respectively.

## 7. 2D $^2\text{H}$ - $^1\text{H}$ NMR spectra of dopamine.HCl

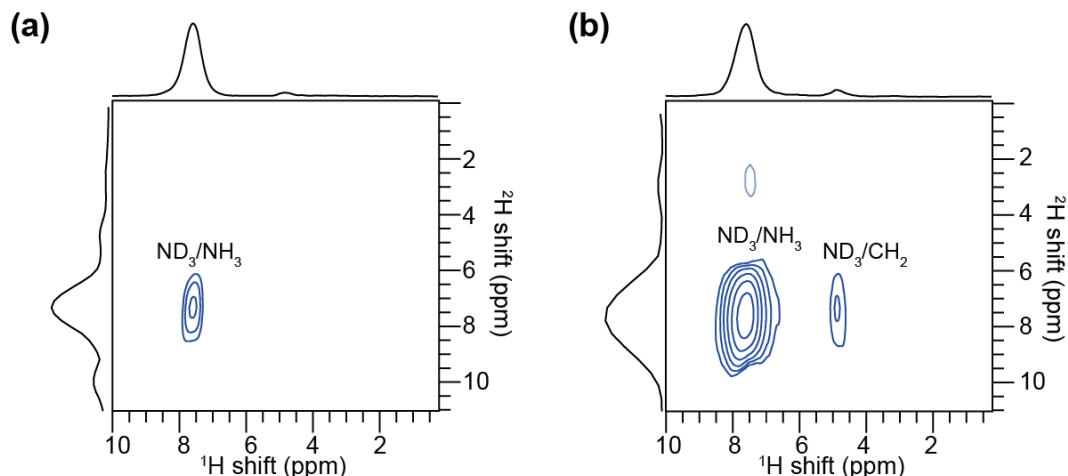


**Figure S9.** Solid-state 2D  $^1\text{H}$ - $^2\text{H}$  HMQC spectra of partially deuterated DOPA acquired with (b)  $\tau_{\text{RCPL}} = 133.2 \mu\text{s}$  and (c)  $\tau_{\text{RCPL}} = 266.5 \mu\text{s}$ , at 18.8 T with 60 kHz MAS.

## 8. Packing interactions in dopamine.HCl

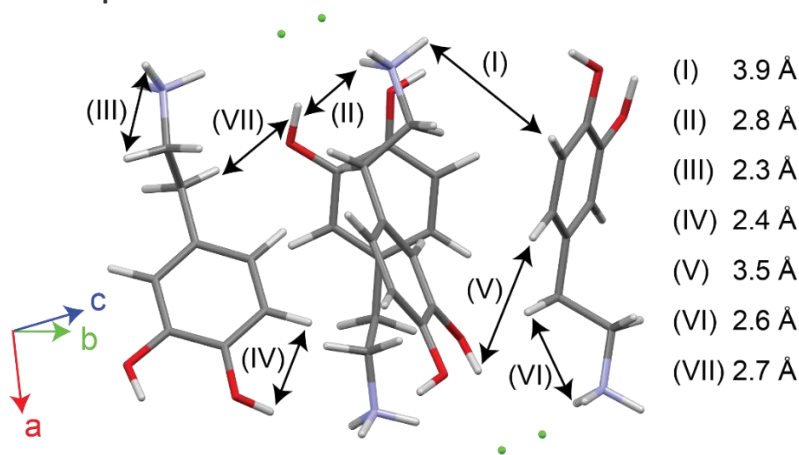


**Figure S10.** Through-space packing interactions contributing to the correlations in the 2D  $^1\text{H}$ - $^2\text{H}$  HMQC spectrum presented in Figure 4d.

**Figure S10** presents the inter- and intramolecular  $^1\text{H}$ - $^2\text{H}$  interactions and the distances between them, as indicated alongside the DFT geometry optimized crystal structure. The intermolecular proximity between the  $\text{ND}_3$  group, the phenolic proton, and a hydroxyl group leads to the 2D peak at 7.8-8.2 ppm ( $^1\text{H}$ ) and 7.0-9.0 ppm ( $^2\text{H}$ ) as indicated by (I) and (II) in Figure 4d and Figure S10. The intramolecular proximity between the  $\text{ND}_3$  group and neighbouring aliphatic  $-\text{CH}_2$  groups (indicated by (III) and (VI)) leads to the signal at 7.0-9.0 ppm ( $^2\text{H}$ ) and 3.5-5.5 ppm ( $^1\text{H}$ ). The intra- and intermolecular proximity of  $\sim 2.4 \text{ \AA}$  and  $\sim 3.5 \text{ \AA}$  between phenolic protons and deuterated hydroxyl groups give rise to the signals indicated by (IV, V) in Figure 4d. The deuterated hydroxyl group is intermolecularly proximate to the  $-\text{CH}_2$  protons, as indicated by (VII) in Figures 4d and S10.

## 9. References

- 1 D. A. Hirsh, A. V. Wijesekara, S. L. Carnahan, I. Hung, J. W. Lubach, K. Nagapudi and A. J. Rossini, *Mol. Pharm.*, 2019, **16**, 3121–3132.
- 2 P. Paluch, A. G. M. Rankin, J. Trébosc, O. Lafon and J. P. Amoureux, *Solid State Nucl. Magn. Reson.*, 2019, **100**, 11–25.
- 3 K. Oda and H. Koyama, *Acta Crystallogr.*, 1972, **B28**, 639–642.
- 4 R. Bergin and D. Carlström, *Acta Crystallogr.*, 1968, **B24**, 1506–1510.
- 5 S. J. Clark, M. D. Segall, C. J. Pickard, P. J. Hasnip, M. I. J. Probert, K. Refson and M. C. Payne, *Zeitschrift für Krist.*, 2005, **220**, 567–570.
- 6 C. J. Pickard and F. Mauri, *Phys. Rev. B*, 2001, **63**, 245101.
- 7 J. R. Yates, C. J. Pickard and F. Mauri, *Phys. Rev. B - Condens. Matter Mater. Phys.*, 2007, **76**, 024401.
- 8 A. Tkatchenko and M. Scheffler, *Phys. Rev. Lett.*, 2009, **102**, 073005.
- 9 D. Vanderbilt, *Phys. Rev. B*, 1990, **41**, 7892.
- 10 P. Raval, J. Trébosc, T. Pawlak, Y. Nishiyama, S. P. Brown and G. N. M. Reddy, *Solid State Nucl. Magn. Reson.*, 2022, **120**, 101808.